Hybrid SDS and WPT-IBBO-DNM Based Model for Ultra-short Term Photovoltaic Prediction

Hui Hwang Goh, *Senior Member*, *IEEE*, Qinwen Luo, Dongdong Zhang, *Member*, *IEEE*, Hui Liu, *Senior Member*, *IEEE*, Wei Dai, *Member*, *IEEE*, Chee Shen Lim, *Senior Member*, *IEEE*, Tonni Agustiono Kurniawan, and Kai Chen Goh

***Abstract*—Accurate photovoltaic (PV) power prediction has been a subject of ongoing study in order to address grid stability concerns caused by PV output unpredictability and intermittency. This paper proposes an ultra-short-term hybrid photovoltaic power forecasting method based on a dendritic neural model (DNM) in this paper. This model is trained using improved biogeography-based optimization (IBBO), a technique that incorporates a domestication operation to increase the performance of classical biogeography-based optimization (BBO). To be more precise, a similar day selection (SDS) technique is presented for selecting the training set, and wavelet packet transform (WPT) is used to divide the input data into many components. IBBO is then used to train DNM weights and thresholds for each component prediction. Finally, each component's prediction results are stacked and reassembled. The suggested hybrid model is used to forecast PV power under various weather conditions using data from the Desert Knowledge Australia Solar Centre (DKASC) in Alice Springs. Simulation results indicate the proposed hybrid SDS and WPT-IBBO-DNM model has the lowest error of any of the benchmark models and hence has the potential to considerably enhance the accuracy of solar power forecasting (PVPF).**

***Index Terms*—Dendritic neural model, improved biogeography-based optimization, photovoltaic power forecasting, similar day selection, wavelet packet transform.**

I. Introduction

UTILIZATION of electrical energy has aided in the evolution of human civilization [1], and industrial activity and daily life cannot function without it. Photovoltaic energy is a frequently used renewable energy source in the power business [2]. Photovoltaic energy generation, on the other hand, is uncertain [3] and cannot be directly connected to the grid. Thus, precisely forecasting ultra-short-term photovoltaic power generation is critical for ensuring steady grid operation following photovoltaic grid connection.

PV power forecast methods can be based on physical or statistical models, the latter of which can be linear or nonlinear in nature [4]. The nonlinear technique, which employs a variety of machine learning algorithms, is frequently used in PV forecasting. Artificial Neural Networks (ANNs) such as Muti-layer Perception (MLP) [5] were used in the early stages of machine learning research for PV forecasting, Support Vector Machine (SVM) [6] and Extreme Learning Machine (ELM) [7] were common. Later, the emphasis has shifted to incorporate algorithms based on deep neural networks, such as Convolutional Neural Network (CNN) [8] and Long Short-term Memory (LSTM) network [9]. However, development of PV prediction models is constrained not just by machine learning model development, but also by model parameter tweaking and data pre-treatment. Currently, a great number of publications [10]–[13] have addressed the topic of parameter tuning by utilizing various optimization algorithms and enhanced versions. Additionally, the performance of photovoltaic energy prediction models is highly dependent on data pre-processing [14]. Numerous data pre-processing techniques exist, for example, Similar Days Analysis [15], Wavelet Transform (WT) [16], Empirical Mode Decomposition [17], etc. Almost all solar forecasting models currently available are hybrid models that incorporate data processing, optimization algorithms, and superior forecasting models [18].

Although deep neural networks are capable of processing large amounts of data and mapping complicated nonlinear relationships, ANNs is still the norm in predicting a single photovoltaic power plant. DNM is a unique single neural network model that exploits the neural dendritic structure's nonlinear processing capabilities to tackle issues such as classification, XOR [19], [20], and so on. Unlike conventional ANNs, this is a true single neuron model capable of nonlinear processing. At the moment, DNM is widely utilized to solve a variety of time series prediction issues, including financial time series predictions [21], crude oil price forecasting [22], very short-term photovoltaic power prediction [23], and wind speed forecasting [24]. While both DNM and traditional ANNs share a fundamental physical structure, DNM requires fewer manual parameters to be set, has a faster convergence rate, and has greater fitting capabilities [25]. However, the typical DNM

Manuscript received June 20, 2021; revised August 11, 2021; accepted September 27, 2021. Date of online publication May 6, 2022; date of current version December 10, 2022. This work was supported in part by Guangxi University (No. A3020051008), and in part by the National Key Research and Development Program of China (No. 2019YFE0118000).

H. H. Goh (corresponding author, email: hhgoh@gxu.edu.cn; ORCID: https://orcid.org/0000-0003-3220-7631), Q. W. Luo, D. D. Zhang, H. Liu, and W. Dai are with the School of Electrical Engineering, Guangxi University, Nanning, Guangxi 530004, China.

C. S. Lim is with the University of Southampton Malaysia, Iskandar Puteri 79200, Malaysia.

T. A. Kurniawan is with the College of the Environment and Ecology, Xiamen University, Fujian 361102, China.

K. C. Goh is with Department of Technology Management, Faculty of Construction Management and Business, University Tun Hussein Onn Malaysia, 86400 Parit Raja, Johor, Malaysia.

DOI: 10.17775/CSEEJPES.2021.04560

based on the BP method has certain drawbacks, including easy-to-fall-into local minima and a greater sensitivity to the initial value [26], [27]. To address this issue, numerous publications [28]–[30] attempt to train DNM using an efficient evolutionary approach to tackle practical engineering issues. BBO is considered a viable tool for preparing DNM for practical work [30]. As a result, this paper examines the application of an enhanced BBO optimization algorithm to train DNM for ultra-short-term photovoltaic forecasting. The IBBO method considers a domestication operation [31] that does not modify the migration and mutation operations of the original BBO algorithm, but works only when the fitness value of BBO remains constant throughout iterations.

On one hand, Zhou *et al*. [7] developed a similar day technique for screening similar days training sets for PVPF using five meteorological variables as characteristics. However, it does not use correlation analysis to discover meteorological elements, which is critical for PVPF, according to [4]. Additionally, Li *et al*. [32] demonstrated that photovoltaic power production is not always comparable across two days with identical meteorological circumstances. This study presents a SDS for accurately simplifying the training set using the European formula in conjunction with expected radiation and historical power data. On the other hand, WT is frequently used to do efficient data preparation in order to increase prediction accuracy [4], [16], [26]. Zhang *et al*. [16] created a PVPF model that combined WT and DNM, confirming that WT increased forecast accuracy marginally in the presence of significant weather fluctuations. However, when solar power and meteorological data contain a greater proportion of high-frequency signals, the decomposition impact of WPT is enhanced [33]. As a result, WPT is utilized to decompose the input variables' time series, resulting in more predictable input data. In terms of experimental development, Leva *et al*. [34] developed a physical hybrid ANN approach for forecasting photovoltaic power over a range of time horizons and resolutions. It is based on publicly available data sets and provides high-precision forecasting results under a variety of weather circumstances. It does, however, present only one day example for each weather condition, similar to [11]. Such experiments are insufficient. We compare the hybrid SDS and WPT-IBBO-DNM prediction model to other benchmark models in this paper and present the results of multiple day's cases under various weather conditions.

The primary contributions of this paper are as follows: 1) Data pre-processing: A SDS approach is developed and then used with WPT to select and deconstruct input data. 2) Prediction model: A dendritic network model is utilized to solve the inadequacies of typical ANNs PV prediction models by utilizing dendritic structure to regulate nonlinear problems. 3) The proposed ultra-short-term hybrid photovoltaic prediction model: The SDS and WPT-IBBO-DNM forecast model, is the first to predict real solar station data using a single dendritic neuron model trained using an effective optimization approach.

The remainder of the paper is organized as follows: Section II delves deeply into data pre-processing techniques such as SDS and WPT. Section III describes the DNM model's structure, the IBBO algorithm, and the IBBO-DNM implementation. Section IV describes the specific prediction process, experimental data, assessment measures, parameters setting, simulation results, and study of computational complexity, as well as the discussion that follows. Finally, Section V highlights the key findings of this paper and discusses future work.

II. Data Preparation

While model selection is critical for PV prediction, data pre-processing and correlation analysis of input and output data are also critical. A good pre-processing strategy reduces not just computational complexity, but also prediction error. This article makes extensive use of the following two data preparation techniques: 1) To accurately simplify training samples, a new comparable day choosing method is applied; 2) The data are decomposed using WPT, which is capable of completely decomposing the photovoltaic variable.

A. Similar Day Selection and Input Selection

While similar day selection is a standard strategy for selecting training sets in photovoltaic prediction, older methods rely heavily on meteorological data such as temperature to find comparable days. Indeed, when power generation is comparable over a two-day period, their temperatures may not be too close [32]. As a result, this paper proposes a new selection strategy based on the Euclidean distance formula. To begin, (1) calculates the historical day with the most similar radiation to the projected day, and then these historical power data that are comparable to the most similar day's power data, are further calculated using the same formula and screened as the training set. The Euclidean distance formula is as follows:

$$D = \sqrt{\sum_{i=1}^{n}(x_i - y_i)^2} \tag{1}$$

where x_i is the power data or radiation data of the history day, and y_i represents the power data or radiation data of the predicted day. n denotes the number of power points in a day.

The Pearson correlation coefficient (PCC) value for each variable with PV power in the data used in this analysis is shown in Table I. The closer the PCC value is to 1, the more strongly correlated the two variables are. It's self-evident that global horizontal radiation (GHR) and diffuse horizontal radiation (DHR) are both critical variables. Although the PCC value for temperature is not very high in this table, temperature is not negligible. As a result, the input variables selected were global horizontal radiation, diffuse horizontal radiation, temperature, and photovoltaic power. PCC value was calculated using the Pearson correlation coefficient formula [7]:

TABLE I
THE PCC VALUE OF EACH VARIABLE WITH PV POWER

Variable	Value	Variable	Value
Temperature	0.155	DHR	0.587
Humidity	−0.133	Wind direction	−0.216
GHR	0.984	–	–

$$PCC = \frac{N\sum_{i=1}^{N} X_i Y_i - \sum_{i=1}^{N} X_i \sum_{i=1}^{N} Y_i}{\sqrt{N\sum_{i=1}^{N} X_i^2 - \left(\sum_{i=1}^{N} X_i\right)^2}\sqrt{N\sum_{i=1}^{N} Y_i^2 - \left(\sum_{i=1}^{N} Y_i\right)^2}} \tag{2}$$

where PCC is the final value, X and Y signify two distinct variables. In this case, X is fixed as the photovoltaic power, while Y is one of the other variables. X_i and Y_i denote the i-th sample value of the corresponding variable, respectively. N is the number of samples of the variable.

B. Wavelet Packet Transform of Input Data

Because WPT is extremely competent at performing time-frequency analysis on signals in engineering applications [26], this work uses it to pre-decompose time series of input variables (photovoltaic power and meteorological data). Not only can WPT decompose the signal's low frequency component, but it can also further decompose the signal's high frequency component. However, because WT can examine just the low frequency component of the signal, the decomposition effect is less than that of WPT when the signal is decomposed into several high frequency signals [33]. When the weather is highly variable, both photovoltaic power and meteorological data contain a large number of high-frequency components.

After the suggested SDS selects the training set, WPT decomposes the time series of each input variable individually. The WPT with three-layer decomposition may theoretically approximate any nonlinear function, allowing for the solution of practical engineering issues [35]. As a result, this paper employs a three-layer WPT to decompose data. The specific three-layer decomposition process is shown in Fig. 1. $W_{1,1}$ and $W_{1,2}$ denote the first layer decomposed results, and $W_{3,1}$–$W_{3,8}$ are the three-layer decompositions. The wavelet basis function is based on the discrete Meyer wavelet and has been shown to be effective in photovoltaic prediction [35]. Due to the fact that it differs in Fourier space by a small carrier, it has a reasonably excellent localization in coordinate space [36].

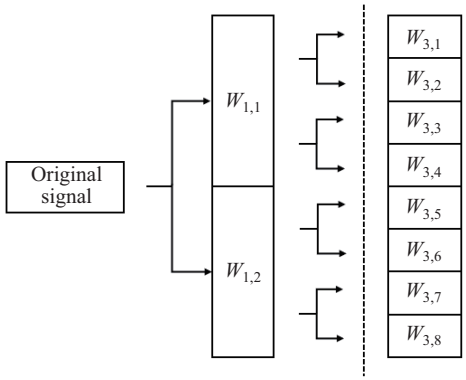

Fig. 1. The three-layer decomposition process of WPT.

III. The IBBO-DNM Prediction Model

A. The Dendritic Neural Model

DNM's topological architecture is distinct from that of other neural networks such as MLP and RBFNN (Radial Basis Function Neural Network). Indeed, MLP achieves nonlinear computation by focusing exclusively on signal propagation between neurons. DNM, on the other hand, is a single neuron model that makes use of the dendritic architecture of neurons to do nonlinear computation. DNM has a faster convergence rate and a higher fitting accuracy than MLP as a result of this unique structure [23], [24].

As shown in Fig. 2, DNM contains four layers: synaptic layer, branch layer, membrane layer, and soma layer [19]. The signal inputs X_1–X_n are first processed through the synaptic layer of each branch for nonlinear calculation, and then summed by each branch to the membrane layer for calculation of output. After membrane layer processing, the signal is transmitted to the soma layer.

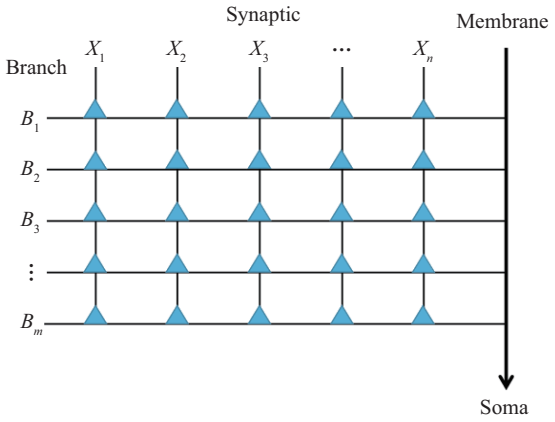

Fig. 2. Structure of the dendritic neural model.

The synaptic layer acts as a kind of gatekeeper for neuronal communication. Each branch's synaptic layer processes the input signals using the sigmoid function. They are then written to the branch layer. The synaptic layer of the i-th input on the j-th branch performs the following processing function [30]:

$$Y_{ij} = \frac{1}{1 + \mathrm{e}^{-k(w_{ij}x_i - \theta_{ij})}} \tag{3}$$

where k is a positive number, defined by the user. w_{ij} and θ_{ij} are the parameters of the i-th input synaptic layer on the j-th branch, determined by the training of the learning algorithm. x_i is the input of the i-th synapse in the range [0, 1].

The branch layer connects the nodes of the synaptic layer and amplifies the synaptic layer signals. Equation (4) describes the multiply operation in the j-th branch [30]:

$$Z_j = \prod_{i=1}^{n} Y_{ij} \tag{4}$$

where Z_j denotes the output of the j-th branch, n is the number of input variables.

The membrane layer connects all the branch layers and sums signals to the soma layer. Here is equation [30]:

$$V = \sum_{j=1}^{M} Z_j \tag{5}$$

where V is the output of the membrane layer, and M is the number of branches.

The results of the membrane layer are conveyed to the soma layer. If they are above a certain threshold, the neuron is activated. Additionally, the sigmoid function is applied to the soma layer, which is expressed in (6) [30]:

$$O = \frac{1}{1 + \mathrm{e}^{-k_s(V-\theta_s)}} \tag{6}$$

where k_s is a user-defined parameter, θ_s represents the threshold and O is the final output of the model.

B. Biogeography-based Optimization

Traditional DNM typically adopts a BP learning algorithm to train its weights and thresholds, but BP algorithm has disadvantages such as easy to be affected by initial value and too slow convergence speed [30]. In order to achieve a better solution to complex problems, such as the photovoltaic power prediction in this paper, it is important to use an efficient and rapid learning algorithm to train DNM. Therefore, this paper adopts IBBO as the learning algorithm for the DNM. BBO simulates migration and drifting of natural species in different geographical regions, so it mainly has two operations: migration and mutation.

The BBO algorithm determines the solution to the problem, referred to as the habitat, based on the habitat suitability index (HSI), and the variable affecting the HSI is referred to as the suitability index variable (SIV) [37]. The migration operation is a critical step in integrating information exchange between habitats and preserving the best SIV in the majority of habitats. Assuming that each solution's migration model is consistent, the migration formulas are as in (7) and (8):

$$\lambda_i = I\left(1 - \frac{n}{Q}\right) \tag{7}$$

$$\mu_i = E\left(\frac{n}{Q}\right) \tag{8}$$

where λ_i and μ_i are the current immigration rate and emigration rate respectively, I and E are the maximum immigration rate and emigration rate respectively, n is the current population quantity, and Q is the maximum population quantity.

Mutation operations alter a range of ecosystems in order to boost species diversity. This mutation technique enables habitats with a low HSI to improve more quickly, while habitats with a high HSI to continue to improve [37]. Even though mutation impairs its HSI, the retained excellent habitats can be protected by an elite approach. The mutation rate mi related to population size can be formulated as follows:

$$m_i = m_{\max}\left(1 - \frac{p_i}{p_{\max}}\right) \tag{9}$$

where $m_{\max}$ is the maximum mutation rate defined by the user, and $P_{\max}$ is the maximum value of individual count probability P_i $(i = 1, 2, \cdots, Q)$.

C. Improved Biogeography-based Optimization

The IBBO includes one more domestication operation compared to normal BBO. An artificial domestication operation is used to expedite the evolution of a species in a certain direction by human intervention. Domestication occurs independently of migration and mutation operations and has no effect on the BBO algorithm's search capability. It becomes effective only when the HSI is at a standstill. Equation (10) describes the process [31]:

$$X_i(j+1) = \begin{cases} X_i(j) - 1, & -1 \le c \le -0.5 \\ X_i(j), & -0.5 < c < 0.5 \\ X_i(j) + 1, & 0.5 \le c \le 1 \end{cases} \tag{10}$$

where $X_i(j)$ is the optimal solution of the population in the j-th iteration, $X_i(j+1)$ is the solution after domestication, and will replace the solution with the low HSI to participate in the subsequent iteration process. c is a random variable with uniform distribution in the interval $[-1, 1]$. Equation (10) implements the nearest rounding through classification discussion. This process simulates a continuous excitation, which randomly selects individuals in the optimal solution to be slightly perturbed. Although the domestication has slight modification to the BBO algorithm itself, the effect is apparent to the algorithms' results.

The following are the steps involved in IBBO training DNM:

1) Initialize IBBO parameters, such as population *popsize*, iteration number *maxgen*, and mutation rate $m_{\max}$.

2) Initialize a collection of randomly generated vector solutions, specifically the habitats in IBBO.

3) Calculate and sort the HSI values, which are equivalent to the mean square error (MSE). The calculation formula is as follows:

$$\mathit{HSI} = \mathit{MSE} = \frac{1}{2N}\sum_{i=1}^{N}(T_i - O_i)^2 \tag{11}$$

where N denotes the number of samples, T_i and O_i represent the target vector and the actual vector of the i-th sample, respectively.

4) Calculate the immigration and emigration rates using (7) and (8), and then carry out the migration and mutation operations according to the probability distribution.

5) Determine whether the convergence process is taking too long. If it is slow, select the optimal domestication solution mentioned before. Otherwise, determine whether the termination condition is satisfied. Otherwise, return to 3).

IV. Case Studies

A. The Specific Prediction Process of the Proposed Model

As mentioned previously, the proposed hybrid SDS and WPT-IBBO-DNM forecasting model is composed primarily of two components: data processing and model prediction. To begin, the proposed SDS is used to select a training set with high quality and an appropriate data size. Next, the input variables' corresponding time series signals are decomposed using three-layer WPT, and the component signals corresponding to each variable are jointly input into the well-trained IBBO-DNM prediction model. Finally, each component's prediction results are stacked and reassembled. The proposed hybrid model's prediction flow chart is depicted in Fig. 3.

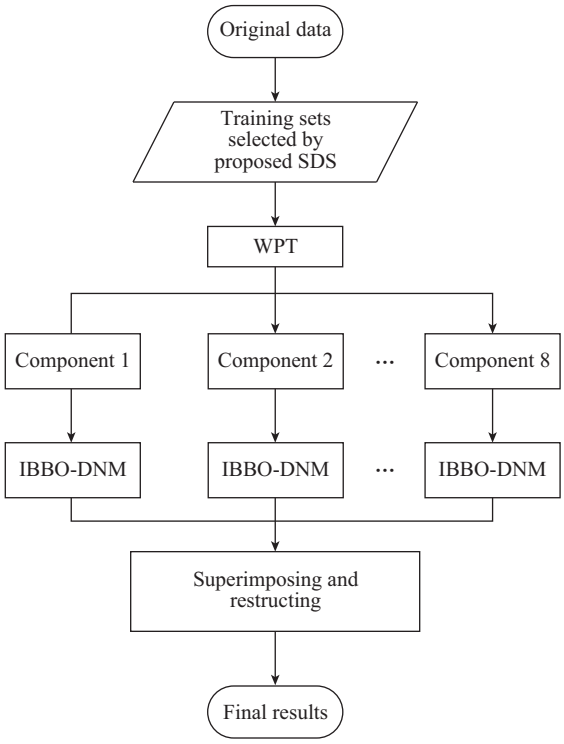

Fig. 3. Prediction flow chart of the proposed hybrid model.

B. Overview of Experimental Data

To validate the proposed hybrid prediction model's performance, a series of tests are conducted using data from the DKASC, Alice Springs photovoltaic system [38]. Table II contains pertinent site information. This article makes use of data spanning the period September 1, 2018 to August 30, 2019, including historical data on electricity generation, temperature, global horizontal radiation, and diffuse horizontal radiation. Among them, data utilized for training, validation, and testing make up 70%, 15%, and 15%, respectively. Due to the limited duration of sunshine, a total of 46 data points from 7:00 to 18:15 in a day were chosen as forecast sample points. The resolution of the data is 15 minutes.

TABLE II
RELEVANT SITE INFORMATION

System specification	Valve
Array Rating	5.04 kW
Panel Rating	280 W
Number of Panels	18
Panel Type	Sungrid SG-280P6
Array Area	35.12 m^2
Inverter Size/Type	6 kW, SMA SMC 6000 A
Installation Completed	Mon, 15 Mar 2010
Array Tilt/Azimuth	Tilt = 20, Azi = 0 (Solar North)

C. Evaluation Metrics

To evaluate the performance of the proposed hybrid prediction model, four evaluation metrics are used to analyze and compare the prediction effects. They are the root mean square error (RMSE), the mean absolute error (MAE), the mean absolute percent error (MAPE), and the correlation coefficient (R^2), respectively. They can be expressed as follows [7], [39]:

$$RMSE = \sqrt{\frac{1}{N}\sum_{i=1}^{N}(P_{f,i} - P_{a,i})^2} \tag{12}$$

$$MAE = \frac{1}{N}\sum_{i=1}^{N}|P_{f,i} - P_{a,i}| \tag{13}$$

$$MAPE = \frac{1}{N}\sum_{i=1}^{N}\left|\frac{P_{f,i} - P_{a,i}}{P_{a,i}}\right| \times 100\% \tag{14}$$

$$R^2 = \frac{\left(N\sum_{i=1}^{N}P_{f,i}P_{a,i} - \sum_{i=1}^{N}P_{f,i}\sum_{i=1}^{N}P_{a,i}\right)^2}{\left[N\sum_{i=1}^{N}P_{f,i}^2 - \left(\sum_{i=1}^{N}P_{f,i}\right)^2\right]\left[N\sum_{i=1}^{N}P_{a,i}^2 - \left(\sum_{i=1}^{N}P_{a,i}\right)^2\right]} \tag{15}$$

where $P_{f,i}$ and $P_{a,i}$ indicate forecasted power value and actual power value at the i-th time point, respectively. N denotes the total number of samples taken for each forecast period.

D. Parameters Setting

As mentioned in Section III, the DNM requires the setting of four user-defined parameters: k, k_s, θ_s and M. However, in this paper, k is equal to k_s. As a result, three parameters must be examined in order to optimize the model's performance. Because attempting each parameter one by one would take an inordinate amount of time, this study employs Taguchi's approach, which has been widely used for the selection of DNM's parameters [25], [30]. L_{16} (4^3) orthogonal arrays of its core parameters are produced, which include only 16 (out of 64) experiments. Table III summarizes the MSEs for 16 different parameter combinations of DNM and the proposed model, where MSE is determined using (11). Each experiment was repeated twenty times, separately, to obtain an average. IBBO's population sizes and iteration times are set to 50 and 1000. To guarantee a fair comparison, all benchmark models use comparable approaches for determining their primary parameters, which are reported in Table IV.

TABLE III
MSES FOR 16 DIFFERENT PARAMETER COMBINATIONS OF DNM AND THE PROPOSED MODEL

No.	$k = k_s$	θ_s	M	DNM	WPT-IBBO-DNM
1	1	2	5	1.31E-03	1.00E-03
2	1	3	10	7.99E-04	3.37E-04
3	1	4	20	7.73E-04	3.28E-04
4	1	5	30	7.18E-04	2.16E-04
5	2	2	10	9.83E-04	3.36E-04
6	2	3	5	5.38E-03	6.97E-04
7	2	4	30	1.08E-03	2.48E-04
8	2	5	20	2.58E-02	4.18E-04
9	3	2	20	1.84E-02	4.57E-04
10	3	3	30	7.78E-03	4.71E-04
11	3	4	5	2.45E-01	9.12E-04
12	3	5	10	2.45E-01	8.81E-04
13	4	2	30	1.47E-02	6.48E-04
14	4	3	20	2.45E-01	4.50E-04
15	4	4	10	2.45E-01	1.72E-03
16	4	5	5	2.45E-01	4.12E-02

Note: The bold values indicate the minimum MSEs for 16 parameter combinations.

TABLE IV
PARAMETERS SETTING OF EACH MODEL

Model	Value
WPT-IBBO-DNM/ IBBO-DNM	$k = k_s = 1$, $\theta_s = 5$, $M = 30$
DNM	$k = k_s = 1$, $\theta_s = 5$, $M = 30$, $\eta = 0.7$ and *maxgen* $= 1000$
Deep Belief Network (DBN)	$M = (10, 5)$, $\eta = 0.1$ and *maxgen* $= 1000$
Elman neural network (ELMAN)	$M = 10$, $\eta = 0.01$ and *maxgen* $= 1000$
General Regression Neural Network (GRNN)	$\eta = 0.3$
MLP	$M = 10$, $\eta = 0.001$ and *maxgen* $= 1000$

where η denotes learning rate, *maxgen* is iteration times, and M of the other models represents the number of hidden layer neurons. It is worth noting that DBN has two hidden layers, so it has two values of M.

E. Simulation Results

In this paper, thorough experiments were undertaken to establish the superiority of the hybrid SDS and WPT-IBBO-DNM prediction model. These prediction tests are implemented on a personal computer with Intel Core i5-6200 and RAM 8.00 GB using MATLAB 2018b. These experiments generally consist of three simulation parts:

1) WPT's Superior Data Decomposition Ability

To demonstrate this, WT-DNM is introduced as a comparison model for WPT-DNM. The results of DNM, WT-DNM, and WPT-DNM prediction under two different weather situations are shown in Table V. Day 1 is a sunny day with low variation in photovoltaic power picked at random from validation data, whereas Day 2 is a cloudy day with significant variation in photovoltaic power selected at random. The two-day test results were chosen to demonstrate the WPT's usefulness in photovoltaic forecast. In this simulation part, WT employs a three-level decomposition technique, whereas WPT employs a two-layer decomposition technique to ensure the number of prediction components is consistent. This contrasts with the suggested three-layer WPT-IBBO-DNM model. It is not difficult to notice from the two-day test that WPT-DNM performs somewhat better than WT-DNM on all four evaluation indices, and both WPT-DNM and WT-DNM perform better than DNM on all four evaluation indexes. This demonstrates that both WPT and WT may enhance prediction outcomes, but WPT's improvement is slightly more than WT's. Additionally, the anticipated performance improvement of WPT-DNM on Day 2 was greater than the predicted performance improvement on Day 1. Specifically, the RMSE of WPT-DNM on Day1 is 0.1273, which is 1.5% lower than the RMSE of WT-DNM. However, on Day 2, WPT-DNM reduced by 4.1% when compared to WT-DNM with the same RMSE value. This demonstrates the importance of using WPT to decompose the model's input data, particularly in the case of extreme weather fluctuations.

TABLE V
COMPARISON OF WT AND WPT'S PERFORMANCE

Model	Criteria	Day1	Day2
DNM	RMSE (kW)	0.1706	0.2094
	MAE (kW)	0.1512	0.1853
	MAPE (%)	0.0451	0.0733
	R^2	0.9950	0.9963
WT-DNM	RMSE (kW)	0.1293	0.1738
	MAE (kW)	0.1123	0.1568
	MAPE (%)	0.0340	0.0569
	R^2	0.9965	0.9962
WPT-DNM	RMSE (kW)	0.1273	0.1667
	MAE (kW)	0.1042	0.1462
	MAPE (%)	0.0274	0.0589
	R^2	0.9953	0.9972

2) IBBO's Efficiency in DNM Model Training

To demonstrate the great efficiency and precision of IBBO, the following algorithms are compared: BBO, Genetic Algorithm (GA), Ant Colony Optimization (ACO), Evolutionary Strategies (ES), Population-Based Incremental Learning (PBIL), and Particle Swarm Optimization (PSO). Fig. 4 depicts the convergence curve for seven algorithms training DNM in PV validation data. MSE is determined using (11) as described in Section III. The parameter values and brief descriptions for each algorithm are listed in Table VI [30], although in this simulation section, population sizes and iteration times are set to 50 and 300, respectively, rather than 50 and 1000. Clearly, the MSE value of IBBO-DNM decreases the fastest and is closest to the ideal solution in the various models during the iteration. Although GA's MSE is tiny during the first 150 iterations, IBBO-DNM's convergence outcome is superior to that of BBO and GA thereafter until the end of the iteration. This indicates that IBBO is a capable and rapid training algorithm for DNM, at least when compared to the other algorithms.

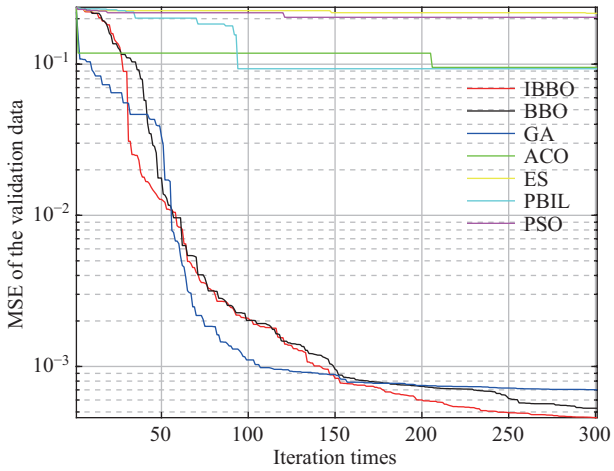

Fig. 4. Comparison of seven algorithm training DNM.

3) The Superiority of the Proposed Hybrid Prediction Model

To demonstrate the suggested model's superiority, this simulation section conducts a series of comparative experiments with numerous advanced models, including MLP, GRNN, ELMAN, DBN, DNM, and IBBO-DNM. The results of the proposed hybrid WPT-IBBO-DNM model's PV power prediction in four distinct weather conditions are displayed in Fig. 5. Clearly, the suggested model's predicted PV power curve is the most similar to the actual PV power curve among four models, regardless of the weather situation. Even when PV power fluctuates significantly (as when it is gloomy or wet),

TABLE VI
EACH ALGORITHM'S SPECIFIC PARAMETER VALUES AND A BRIEF DESCRIPTION [30]

Algorithm	Brief introduction	Parameter	Value
BBO/IBBO	Details show in Section III.	Habitat modification probability	1
		Immigration probability bounds per gene	[0, 1]
		Step size for numerical integration of probability	1
		Max immigration and max emigration	1
		Mutation probability	0.005
PSO	PSO mimics the search behavior of a bird swarm.	Topology	Fully connected
		Cognitive constant	1
		Social constant	1
		Inertia constant	0.3
GA	GA is simulation of natural selection.	Type	Real coded
		Selection	Roulette wheel
		Crossover	Single point (probability = 1)
		Mutation	Uniform (probability = 0.01)
ACO	ACO emulates the foraging behavior of ants to search the shortest route between a food source and their nest.	Initial pheromone	1e-6
		Pheromone update constant	20
		Pheromone constant	1
		Global pheromone decay rate	0.9
		Local pheromone decay rate	0.5
		Pheromone sensitivity	1
		Visibility sensitivity	5
ES	ES is inspired by the concept of the evolution.	Number of offspring	10
		Standard deviation	1
PBIL	PBIL is a generalization of a univariate marginal distribution algorithm.	Learning rate	0.05
		Good population member	1
		Bad population member	0
		Elitism parameter	1
		Mutation probability	0.1

the model's forecast results remain satisfactory. Notably, all models provide rather accurate forecasts on sunny days. However, as weather conditions change, particularly on overcast and wet days, the suggested model's prediction curve remains close to the real power, in contrast to the other models.

In order to further compare the prediction performance of the proposed model with other models, the RMSE, MAE, MAPE and R^2 values of 7 models are shown in Table VII. It demonstrates the suggested hybrid model outperforms the other benchmark models, achieving the lowest average RMSE = 0.0693 kW, MAE = 0.0548 kW, MAPE = 3.2444%, and the highest average R^2 = 0.9947%. The MAPE value of the suggested model is significantly lower than of other models, particularly on wet days. In all weather scenarios, IBBO-DNM model values are slightly less than DNM values. For example, when compared to the average RMSE of the DNM model, the IBBO-DNM model's RMSE is lowered by around 11.7%. It reveals that IBBO is capable of fully utilizing DNM, but typical BP training drastically inhibits its performance. DBN also outperforms DNM in terms of prediction accuracy because of its deep neural network topology, however it is still somewhat worse than IBBO-DNM. DNM's average MAE is 8.7% greater than DBN's, but IBBO DNM's average MAPE is 4.5% lower than DBN's. However, DNM clearly outperforms MLP, GRNN and ELMAN when it comes to simple neural network models.

Figure 6 provides a logical explanation for the RMSE, MAE, and MAPE results for the seven forecast models under various weather conditions. That Figure is self-evident. Fig. 6(a) and Fig. 6(b) have a nearly same change in that all models have the highest error value on cloudy days, implying that forecast accuracy is lowest on cloudy days. However, on rainy days, the RMSE and MAE values are considerably lower than on sunny days, because the maximum power value on sunny days is significantly greater than on rainy days. Fig. 6(c) confirms this (Fig. 6(c) has changed the order of x-axis). Sunny days have the lowest MAPE, which means they have the best prediction impact. It is worth mentioning the suggested model's MAPE improves significantly on rainy days, indicating the model's superiority on rainy days. Moreover, the proposed model has the least variation range across all the models under various weather situations, indicating the proposed model has some stability. Additionally, Fig. 7 depicts the histogram of the 14 test days' error distribution for all sorts of weather in this simulation part. Following calculation, roughly 85% of the error is contained within the range [−0.1, 0.1].

F. Computational Complexity Analysis

The suggested model is primarily composed of DNM, and the computational complexity of IBBO must be addressed. To begin, the computational complexity of the DNM neural network model can be equated to the number of training parameters [25]. Specifically, DNM has $2 * I * M$ parameters, where I is the feature number and M represents the number of dendritic branches. So DNM's complexity is $O(I * M^2)$. Similarly, for IBBO, its computation complexity can be expressed as $O(E * N^2)$, where E denotes iteration times and N is population size. Table VIII summarizes the time required for each model to forecast 46 points in a single day. As a result, the proposed model has the longest run time of all of the models in Table VIII. However, given the increasing popularity

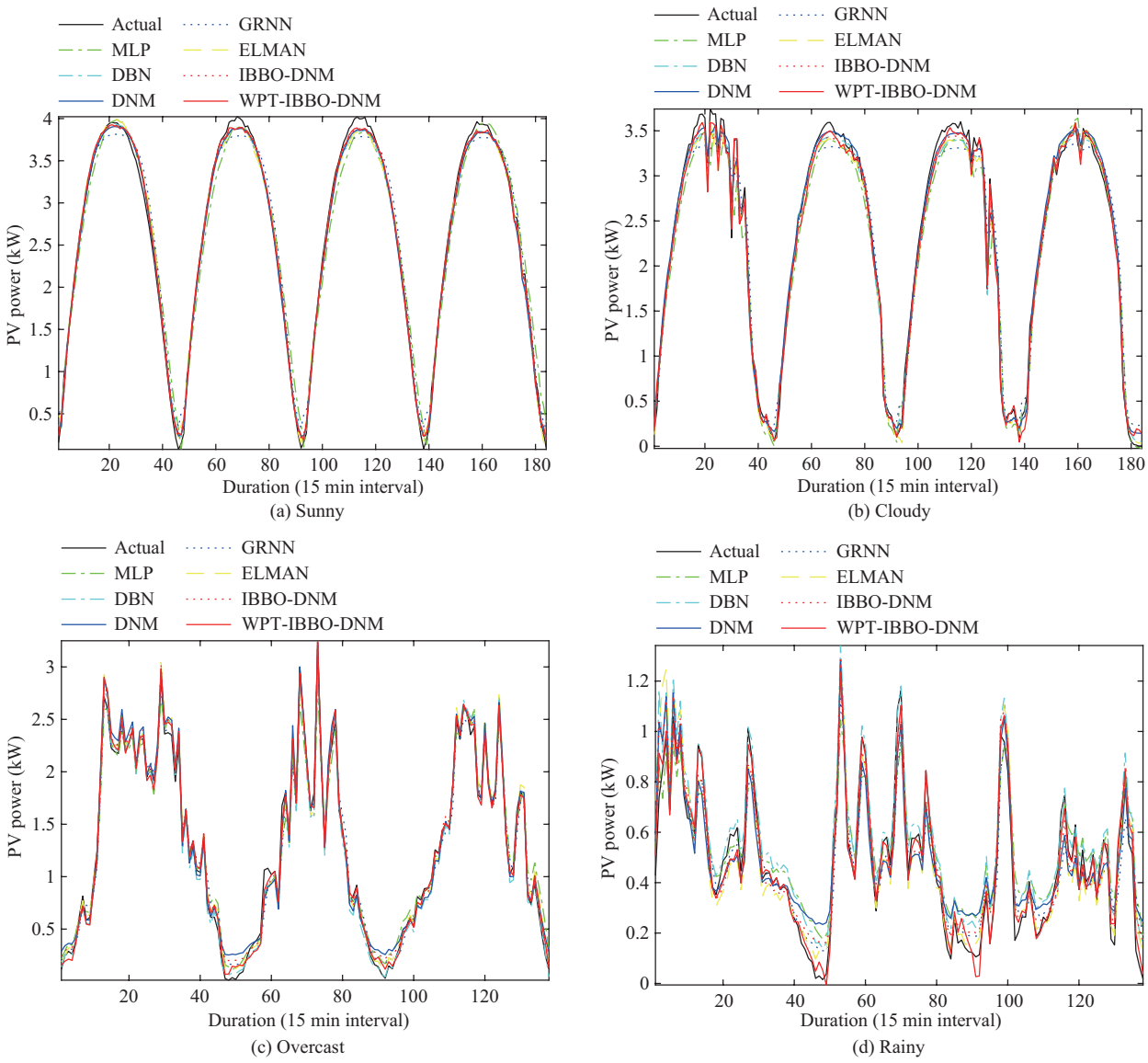

Fig. 5. Prediction results of 7 models in different weather.

of high-performance cloud servers and GPUs, the proposed model retains a high degree of practical utility. Furthermore, as illustrated in Fig 8, the suggested model achieved the ultimate MSE value for MLP and DNM in fewer than 100 iterations, implying that it may not require as much running time in practice.

G. Discussion

In a nutshell, the hybrid SDS and WPT-IBBO-DNM model outperforms the other models in all four weather conditions evaluated in this work, demonstrating the suggested model is a powerful PV power forecasting model. In terms of data processing, WPT was used to address the fault of WT in that it could not further breakdown high-frequency components, and the experiment confirmed that its decomposition capacity improved prediction accuracy. In terms of prediction models, while both DNM and MLP use the BP algorithm for training, DNM has a higher prediction efficiency. This demonstrates the strength of the DNM network structure. MLP contains a large number of parameters that must be set manually, and there is no efficient way to do it. While DNM can address some of MLP's faults, it also suffers from inadequacy of the BP method. BBO is a highly effective DNM training technique that has been proved in [30]. As a result, an enhanced BBO that takes domestication into account is utilized to train DNM in this paper, and trials demonstrate its performance when compared to many other methods.

V. Conclusion

The hybrid SDS and WPT-IBBO-DNM forecast models are proposed in this research as a unique model for ultra-short-term hybrid photovoltaic forecasting. This paper's primary objective is as follows: 1) A SDS approach is developed that incorporates the European formula, anticipated radiation, and historical power data in order to address the issue of previous SDS screening training sets being inaccurate; 2) WPT is used to breakdown input data in order to get greater forecast

TABLE VII
EVALUATION METRICS OF 7 MODELS IN DIFFERENT WEATHER

Method	Criteria	Sunny	Cloudy	Overcast	Rainy	Average
MLP	RMSE (kW)	0.1771	0.2169	0.1870	0.1112	0.1731
	MAE (kW)	0.1524	0.1669	0.1471	0.0934	0.1400
	MAPE (%)	4.1952	6.2197	7.9010	13.2378	7.8884
	R^2	0.9918	0.9871	0.9822	0.9673	0.9821
GRNN	RMSE (kW)	0.1468	0.2070	0.1071	0.0952	0.1390
	MAE (kW)	0.1273	0.1599	0.0855	0.0744	0.1118
	MAPE (%)	3.5744	5.5058	4.2104	12.2097	6.3751
	R^2	0.9951	0.9877	0.9922	0.9505	0.9814
ELMAN	RMSE (kW)	0.0945	0.1208	0.0887	0.0962	0.1001
	MAE (kW)	0.0766	0.0925	0.0687	0.0769	0.0787
	MAPE (%)	2.4535	3.4788	4.0590	14.0752	6.0166
	R^2	0.9977	0.9966	0.9950	0.9392	0.9821
DBN	RMSE (kW)	0.0806	0.1056	0.0789	0.0957	0.0902
	MAE (kW)	0.0645	0.0865	0.0635	0.0804	0.0737
	MAPE (%)	1.9398	3.2114	3.6820	11.0623	4.9739
	R^2	0.9983	0.9972	0.9966	0.9517	0.9860
DNM	RMSE (kW)	0.0793	0.1088	0.1041	0.1038	0.0990
	MAE (kW)	0.0667	0.0868	0.0815	0.0853	0.0801
	MAPE (%)	2.0642	3.0713	3.8918	12.2873	5.3287
	R^2	0.9986	0.9961	0.9932	0.9370	0.9812
IBBO-DNM	RMSE (kW)	0.0769	0.1033	0.0876	0.0817	0.0874
	MAE (kW)	0.0623	0.0804	0.0696	0.0672	0.0699
	MAPE (%)	1.8512	2.8983	3.4379	10.8082	4.7489
	R^2	0.9983	0.9973	0.9952	0.9566	0.9869
WPT-IBBO-DNM	RMSE (kW)	0.0700	0.0924	0.0675	0.0471	0.0693
	MAE (kW)	0.0548	0.0755	0.0529	0.0361	0.0548
	MAPE (%)	1.6143	2.6411	2.8714	5.8507	3.2444
	R^2	0.9986	0.9978	0.9969	0.9856	0.9947

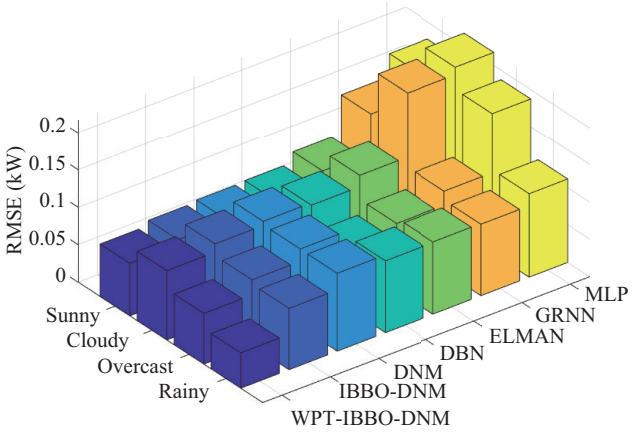

(a) RMSE

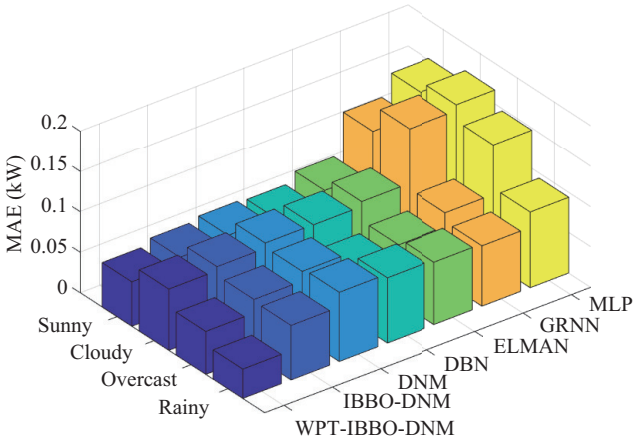

(b) MAE

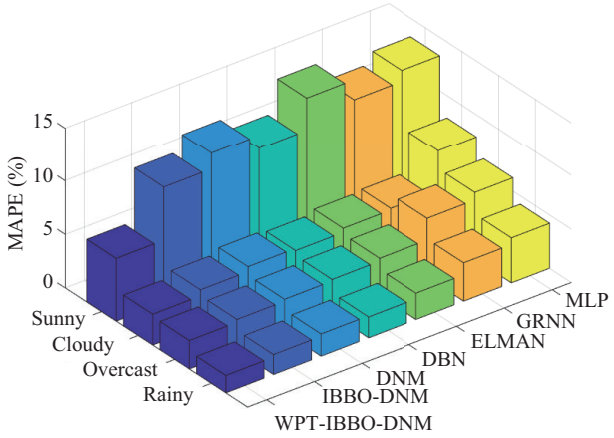

(c) MAPE

Fig. 6. RMSE, MAE, MAPE values of 7 models under different weather.

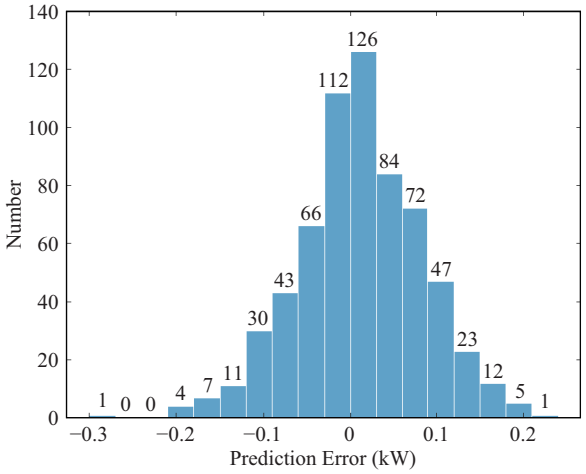

Fig. 7. Error distribution of all 14 test days.

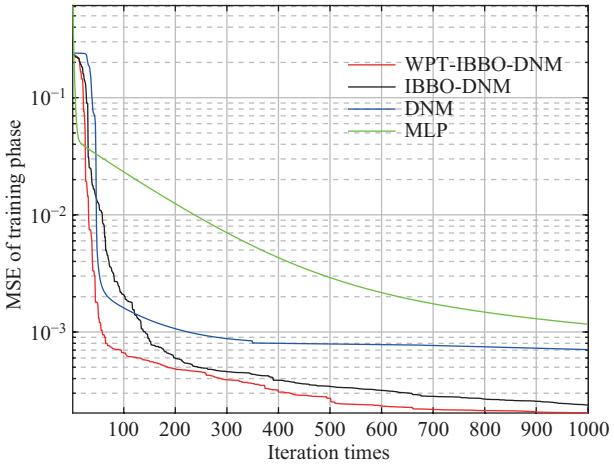

Fig. 8. The convergence curve of the hybrid proposed model.

TABLE VIII
EXECUTION TIME OF EACH MODEL

Model	Time (s)	Model	Time (s)
Proposed	356.23	ELMAN	12.01
DNM	22.68	GRNN	3.69
DBN	18.31	GRNN	6.49

precision. This addresses the disadvantage of WT in that it cannot further decompose high-frequency components of photovoltaic power; 3) Due to the excellent efficacy of BBO in training, BBO integrated with domestication operation (IBBO) is used to train DNM and then used to real PV station data prediction.

To be more precise, we use SDS to pick the training set and WPT to deconstruct the input data into various components. Following that, IBBO develops DNM weights and thresholds. Following that, each component is mapped to the input of the trained IBBO-DNM, and projected outcomes are superimposed and recreated. Finally, WPT-IBBO-DNM was evaluated in a variety of weather conditions and the outcomes were compared to MLP, DNM, and WPT-DNM. Results indicate the suggested hybrid forecast model has the best RMSE, MAE, MAPE, and R^2 values. As a result, it is stated the proposed SDS and WPT-IBBO-DNM-based prediction model has the potential to increase accuracy of PV power forecasting, hence contributing to optimization of real-time power dispatch and grid stability.

The future research direction will be on how to efficiently train DNM with optimization algorithms for application to more difficult multi-dimensional time series prediction problems, as well as how to efficiently and accurately pick user-defined parameters for DNM. Indeed, this article is the first to forecast multi-variable dimensional time series using DNM, which is distinct from earlier DNM studies. This is the model's restriction. To achieve reliable prediction of multi-variable photovoltaic time series, we increase the number of dendritic branches in DNM and employ an optimization approach. Both of these factors contribute to the model's increased running duration.

REFERENCES

[1] Z. F. Guo, K. L. Zhou, C. Zhang, X. H. Lu, W. Chen, and S. L. Yang, "Residential electricity consumption behavior: Influencing factors, related theories and intervention strategies," *Renewable and Sustainable Energy Reviews*, vol. 81, pp. 399–412, Jan. 2018.

[2] A. K. Raturi, "Renewables 2019 global status report," REN21, Paris, France, 2019.

[3] M. Z. Pan, C. Li, R. Gao, Y. T. Huang, H. You, T. S. Gu, and F. R. Qin, "Photovoltaic power forecasting based on a support vector machine with improved ant colony optimization," *Journal of Cleaner Production*, vol. 277, pp. 123948, Dec. 2020.

[4] R. Ahmed, V. Sreeram, Y. Mishra, and M. D. Arif, "A review and evaluation of the state-of-the-art in PV solar power forecasting: Techniques and optimization," *Renewable and Sustainable Energy Reviews*, vol. 124, pp. 109792, May 2020.

[5] I. Parvez, A. Sarwat, A. Debnath, T. Olowu, M. G. Dastgir, and H. Riggs, "Multi-layer perceptron based photovoltaic forecasting for rooftop PV applications in smart grid," in *2020 SoutheastCon*, 2020, pp. 1–6.

[6] J. Shi, W. J. Lee, Y. Q. Liu, Y. P. Yang, and P. Wang, "Forecasting power output of photovoltaic systems based on weather classification and support vector machines," *IEEE Transactions on Industry Applications*, vol. 48, no. 3, pp. 1064–1069, May/Jun. 2012.

[7] Y. Zhou, N. R. Zhou, L. H. Gong, and M. L. Jiang, "Prediction of photovoltaic power output based on similar day analysis, genetic algorithm and extreme learning machine," *Energy*, vol. 204, pp. 117894, Aug. 2020.

[8] J. C. Yan, L. Hu, Z. Zhen, F. Wang, G. Qiu, Y. Li, L. Z. Yao, M. Shafie-Khah, and J. P. S. Catalão, "Frequency-domain decomposition and deep learning based solar PV power ultra-short-term forecasting model," *IEEE Transactions on Industry Applications*, vol. 57, no. 4, pp. 3282–3295, Jul./Aug. 2021.

[9] M. S. Hossain and H. Mahmood, "Short-term photovoltaic power forecasting using an LSTM neural network and synthetic weather forecast," *IEEE Access*, vol. 8, pp. 172524–172533, 2020.

[10] M. K. Chai, F. Xia, S. T. Hao, D. G. Peng, C. G. Cui, and W. Liu, "PV power prediction based on LSTM with adaptive hyperparameter adjustment," *IEEE Access*, vol. 7, pp. 115473–115486, 2019.

[11] Z. F. Liu, L. L. Li, M. L. Tseng, and M. K. Lim, "Prediction short-term photovoltaic power using improved chicken swarm optimizer - Extreme learning machine model," *Journal of Cleaner Production*, vol. 248, pp. 119272, Mar. 2020.

[12] M. K. Behera and N. Nayak, "A comparative study on short-term PV power forecasting using decomposition based optimized extreme learning machine algorithm," *Engineering Science and Technology, an International Journal*, vol. 23, no. 1, pp. 156–167, Feb. 2020.

[13] L. L. Li, X. Zhao, M. L. Tseng, and R. R. Tan, "Short-term wind power forecasting based on support vector machine with improved dragonfly algorithm," *Journal of Cleaner Production*, vol. 242, pp. 118447, Jan. 2020.

[14] U. K. Das, K. S. Tey, M. Seyedmahmoudian, S. Mekhilef, M. Y. I. Idris, W. Van Deventer, B. Horan, and A. Stojcevski, "Forecasting of photovoltaic power generation and model optimization: A review," *Renewable and Sustainable Energy Reviews*, vol. 81, pp. 912–928, Jan. 2018.

[15] Y. Zhang, M. Beaudin, R. Taheri, H. Zareipour, and D. Wood, "Day-ahead power output forecasting for small-scale solar photovoltaic electricity generators," *IEEE Transactions on Smart Grid*, vol. 6, no. 5, pp. 2253–2262, Sep. 2015.

[16] H. Liu, X. W. Mi, and Y. F. Li, "Wind speed forecasting method based on deep learning strategy using empirical wavelet transform, long short term memory neural network and elman neural network," *Energy Conversion and Management*, vol. 156, pp. 498–514, Jan. 2018.

[17] D. X. Niu, K. K. Wang, L. J. Sun, J. Wu, and X. M. Xu, "Short-term photovoltaic power generation forecasting based on random forest feature selection and CEEMD: A case study," *Applied Soft Computing*, vol. 93, pp. 106389, Aug. 2020.

[18] Q. Z. Liu, Y. B. Shen, L. Wu, J. Li, L. R. Zhuang, and S. F. Wang, "A hybrid FCW-EMD and KF-BA-SVM based model for short-term load forecasting," *CSEE Journal of Power and Energy Systems*, vol. 4, no. 2, pp. 226–237, Jun. 2018.

[19] T. Jiang, D. Z. Wang, J. K. Ji, Y. Todo, and S. C. Gao, "Single dendritic neuron with nonlinear computation capacity: A case study on XOR problem," in *2015 IEEE International Conference on Progress in Informatics and Computing (PIC)*, 2015, pp. 20–24.

[20] Y. Todo, H. Tamura, K. Yamashita, and Z. Tang, "Unsupervised learnable neuron model with nonlinear interaction on dendrites," *Neural Networks*, vol. 60, pp. 96–103, Dec. 2014.

[21] J. K. Ji, S. C. Gao, J. J. Cheng, Z. Tang, and Y. Todo, "An approximate logic neuron model with a dendritic structure," *Neurocomputing*, vol. 173, pp. 1775–1783, Jan. 2016.

[22] T. L. Zhou, S. C. Gao, J. H. Wang, C. Y. Chu, Y. Todo, and Z. Tang, "Financial time series prediction using a dendritic neuron model," *Knowledge-Based Systems*, vol. 105, pp. 214–224, Aug. 2016.

[23] S. Wang, D. Sugiyama, J. Sun, L. Yang, and S. C. Gao, "Dendritic neuron model trained by biogeography-based optimization for crude oil price forecasting," in *2018 10th International Conference on Intelligent Human-Machine Systems and Cybernetics (IHMSC)*, 2018, pp. 36–40.

[24] K. W. Zhao, T. F. Zhang, X. L. Lai, C. X. Dou, and D. Yue, "A dendritic neuron based very short-term prediction model for photovoltaic power," in *2018 Chinese Control And Decision Conference (CCDC)*, 2018, pp. 1106–1110.

[25] Z. Y. Song, Y. J. Tang, J. K. Ji, and Y. Todo, "Evaluating a dendritic neuron model for wind speed forecasting," *Knowledge-Based Systems*, vol. 201–202, pp. 106052, Aug. 2020.

[26] T. F. Zhang, C. F. Lv, F. M. Ma, K. W. Zhao, H. K. Wang, and G. M. P. O'Hare, "A photovoltaic power forecasting model based on dendritic neuron networks with the aid of wavelet transform," *Neurocomputing*, vol. 397, pp. 438–446, Jul. 2020.

[27] M. K. Weir, "A method for self-determination of adaptive learning rates in back propagation," *Neural Networks*, vol. 4, no. 3, pp. 371–379, 1991.

[28] A. Van Ooyen and B. Nienhuis, "Improving the convergence of the back-propagation algorithm," *Neural Networks*, vol. 5, no. 3, pp. 465–471, 1992.

[29] S. Wang, Y. Yu, L. Zou, S. Li, H. Yu, Y. Todo, and S. C. Gao, "A novel median dendritic neuron model for prediction," *IEEE Access*, vol. 8, pp. 192 339– 192 351, 2020.

[30] S. C. Gao, M. C. Zhou, Y. R. Wang, J. J. Cheng, H. Yachi, and J. H. Wang, "Dendritic neuron model with effective learning algorithms for classification, approximation, and prediction," *IEEE Transactions on Neural Networks and Learning Systems*, vol. 30, no. 2, pp. 601–614, Feb. 2019.

[31] Q. Wang, J. Chen, Q. S. Li, and J. C. Liu, "PID parameter optimization based on improved biogeography-based optimization algorithm," *Jour-*

nal of Nanjing University of Science and Technology, vol. 41, no. 4, pp. 519–525, Aug. 2017.
[32] Q. Li, X. Y. Zhang, T. J. Ma, C. L. Jiao, H. Wang, and W. Hu, "A multi-step ahead photovoltaic power prediction model based on similar day, enhanced colliding bodies optimization, variational mode decomposition, and deep extreme learning machine," *Energy*, vol. 224, pp. 120094, Jun. 2021.
[33] H. Liu and C. Chen, "Data processing strategies in wind energy forecasting models and applications: A comprehensive review," *Applied Energy*, vol. 249, pp. 392–408, Sep. 2019.
[34] S. Leva, A. Nespoli, S. Pretto, M. Mussetta, and E. G. C. Ogliari, "PV plant power nowcasting: A real case comparative study with an open access dataset," *IEEE Access*, vol. 8, pp. 194428–194440, 2020.
[35] Y. Yang, "Study on short-term probability interval prediction of photovoltaic power based on wavelet packet theory," M.S. thesis, Department, Northeast Electric Power University, Jilin, China, 2020.
[36] N. A. Leontiev and A. G. Nyurova, "The use of discrete meyer wavelet for speech segmentation," in *2019 International Multi-Conference on Industrial Engineering and Modern Technologies (FarEastCon)*, 2019, pp. 1–3.
[37] D. Simon, "Biogeography-based optimization," *IEEE Transactions on Evolutionary Computation*, vol. 12, no. 6, pp. 702–713, Dec. 2008.
[38] *Data Download | DKA Solar Centre*, Accessed: Sep.2, 2019. [Online]. Available: http://dkasolarcentre.com.au/locations/alice-springs
[39] P. J. Lin, Z. N. Peng, Y. F. Lai, S. Y. Cheng, Z. C. Chen, and L. J. Wu, "Short-term power prediction for photovoltaic power plants using a hybrid improved Kmeans-GRA-Elman model based on multivariate meteorological factors and historical power datasets," *Energy Conversion and Management*, vol. 177, pp. 704–717, Dec. 2018.

Hui Hwang Goh (SM'12) received the B.Eng. (hons.), M.Eng., and Ph.D. degrees in Electrical Engineering from the Universiti Teknologi Malaysia, Johor Bahru, Malaysia, in 1998, 2002, and 2007, respectively. He is currently a Professor of Electrical Engineering with the School of Electrical Engineering, Guangxi University, Nanning, China. His research interests include embedded power generation modeling and simulation, power quality studies, wavelet analysis, multicriteria decision-making, renewable energies, and dynamic equivalent. Dr. Goh is a Fellow of the Institution of Engineering and Technology, U.K. He is also a Fellow of the ASEAN Academy of Engineering and Technology, Chinese Society of Electrical Engineering (CSEE), and the Institution of Engineers, Malaysia, a Chartered Engineer under the Engineering Council United Kingdom, and a Professional Engineer under the Board of Engineers, Malaysia.

Qinwen Luo received the B.S. degree in Electrical Engineering and Its Automation from Southwest University of Science and Technology, Mianyang, China, in 2019. He is currently pursuing the M.S. degree at the School of Electrical Engineering, Guangxi University. His current research directions include artificial intelligence, machine learning, and photovoltaic power forecasting.

Dongdong Zhang (M'17) received the B.Eng. degree in Electrical Engineering and Automation from the College of Electrical Engineering, Qilu University of Technology, Shandong, China, in 2013, received the M.S. degree in Electric Power System and Automation from North China Electric Power University in 2016, and received the Ph.D. degree in Electrical Engineering at the Xi'an Jiaotong University in 2019. Currently, he is an Assistant Professor with Guangxi University. His research interests include the modeling and optimization of multiple energy system, energy market, and electrical machines and its driving system design.

Hui Liu (M'12–SM'17) received his M.S. degree in 2004 and Ph.D. degree in 2007 from the College of Electrical Engineering at Guangxi University, China, both in Electrical Engineering. He worked in Tsinghua University as a postdoctoral fellow from 2011 to 2013 and in Jiangsu University as a faculty member from 2007 to 2016. He visited the Energy Systems Division at Argonne National Laboratory, Argonne, IL, USA, from 2014 to 2015. He joined the School of Electrical Engineering at Guangxi University in 2016, where he is a Professor and Deputy Dean. He is an Editor of the IEEE Transactions on Smart Grid and the IEEE PES Letters. He is also an Associate Editor of the IET Smart Grid and the IET Generation, Transmission & Distribution. His research interests include power system optimization, power system stability and control, electric vehicles, integrated energy systems, demand response, etc.

Wei Dai (M'19) received the Ph.D. degree in Electrical Engineering from Chongqing University, in 2018. He currently works as an Assistant Professor with Guangxi University. His research interests include multiple energy systems, power systems analysis, renewable energy, and large-scale system problems.

Chee Shen Lim (Senior Member, IEEE) received the B.Eng. (Hons.) degree in Electrical Engineering from the University of Malaya, Kuala Lumpur, Malaysia, in 2009, and the joint-university Ph.D. degrees in Power Electronics and Drives from the university of Malaya, Kuala Lumpur, and Liverpool John Moores University, Liverpool, U.K., in 2013.

From 2013 to 2015, he was a Research Scientist with the Experimental Power Grid Centre, Agency for Science, Technology and Research, Singapore. From 2015 to 2021, he was an Assistant/Associate Professor of electrical and electronic engineering with the University of Southampton Malaysia Campus. He is currently an Associate Professor of electrical and electronic engineering with Xi'an Jiaotong-Liverpool University, China. Dr. Lim serves currently as an Associate Editor of the IET Electric Power Applications.

Tonni Agustiono Kurniawan is an Associate Professor at Xiamen University, China. Prior to joining the University, he was a scholar at United Nations University (Tokyo). He got his Ph.D. degree from the Hong Kong Polytechnic University, Hong Kong, China. Significant contribution to research in the field has earned him recognition from the World Economic Forum (Switzerland). So far Kurniawan has been cited over 10,500 times with a Hirsch factor of 40 (Scopus). Since 2011, the Institute for Scientific Information Thompson Reuters has identified him among the top 1% of researchers in the field of Engineering according to the Essential Science Indicators of Web of Knowledge.

Kai Chen Goh is an Associate Professor in Faculty of Technology Management and Business at Universiti Tun Hussein Onn Malaysia, Malaysia. He received his Ph.D. degree in Built Environment and Engineering from Queensland University of Technology, M.S. degree in Construction Management, B.Sc. Degree (Hons) in Construction, and Diploma in Quantity Surveying from Universiti Teknologi Malaysia.